RSC Advances

PAPER

View Article Online
View Journal | View Issue

Cite this: *RSC Adv.*, 2020, **10**, 36897

Selective extraction and determination of beryllium in real samples using amino-5,8-dihydroxy-1,4-naphthoquinone functionalized magnetic MIL-53 as a novel nanoadsorbent†

Soheyla Rezabeyk and Mahboobeh Manoochehri *

Herein, a magnetic MOF for preconcentration of Be(II) was synthesized. The material is obtained from magnetite (Fe_3O_4) nanoparticles that were modified with 2-amino-5,8-dihydroxy-1,4-naphthoquinone (ADHNQ) and then reacted with terephthalic acid and iron(III) chloride to form a metal–organic framework of the type MIL-53(Fe) capable of extracting Be(II). The extraction parameters were optimized by employing design of experiments methodology. Beryllium concentration was determined by flame atomic absorption spectrometry (FAAS). The detection limit was as low as 0.07 ng mL^{-1} and the quantification limit is 0.2 ng mL^{-1}. Linearity extends from 0.2 to 100 ng mL^{-1}, and the precision of the method (intra and inter-day assay) is <9.5%. The recoveries of real sample analysis were in the range of 89–101%. The method was successfully applied to the analysis of various real water samples and an alloy sample.

Received 20th June 2020
Accepted 12th September 2020

DOI: 10.1039/d0ra05408a

rsc.li/rsc-advances

1 Introduction

Beryllium (Be) as one of the lightest (three times lighter than aluminium) and strongest metals (six times harder than steel) is a strategic metal because of its vital importance and applications in several industries.[1,2] Pure Be and its alloys with some metals, including Ni, Cu, Mg and Al, have been applied in aerospace components, electronic instrumentation, electrical equipment, the automotive industry, the nuclear industry, jewelry, ceramics, dental amalgams and prostheses.[1,3] Beryllium and its compounds can cause acute toxicity with the lungs as the target organ in human beings. As early as the 1930s, in beryllium extraction and processing industries, the cases of acute beryllium disease were reported as an inflammation of the respiratory tract.[1] Beryllium exposure takes place through inhalation and ingestion.[1] However, the mechanism of chronic beryllium disease is not thoroughly known. Probably Be combines with special proteins such as ferritin, then enters into the lungs and is taken up by macrophages of the lungs, subsequently causing lesions in the lungs.[3] The water supplies and environment are mainly contaminated due to the discharges of related industries and also due to burning coal, while Be exists in the earth crust in the range of ~2.8–5.0 μg g^{-1}.[4] It has been reported that many serious and fatal problems can occur due to the contamination of Be and its compounds, below 4 μg L^{-1} in waters. Based on various national guidelines, the concentration of Be(II) in tap and surface water should not exceed a limit of 0.1 μg L^{-1} and 0.2 μg L^{-1}, respectively.[5] Generally, in natural water, the average concentration of Be(II) is in the range of ng L^{-1}.[6] As International Agency for Research on Cancer (IARC) states, Be and its compounds are classified as group 1 due to their carcinogenic effect to human and animal.[7] Thus, it is necessary to develop and apply highly accurate and sensitive methods for determination of Be(II) at very low concentrations. The techniques applied for Be(II) determination are as follows: atomic absorption spectrometry (AAS),[6] spectrofluorimetry,[8] spectrophotometric method,[16] inductively coupled plasma mass spectrometry,[9] inductively coupled plasma optical emission spectrometric detection[10] and gas chromatography.[11]

Solid phase extraction (SPE) has been considered as one of the principal sample preparation methods due to its merits, including easy configuration, high enrichment factors and recoveries, low cost and facile on-line hyphenation.[5] Magnetic solid-phase extraction (MSPE) is a type of SPE in dispersion mode utilizing magnetic adsorbents which has triggered interest in sample pretreatment strategies due to its unique magnetic behavior, facile implementation and low cost. It is necessary to consider the nature, features and behavior of the magnetic adsorbent in the MSPE adsorbent development.[12,13] Thus, diverse adsorbent have been introduced for the extraction of various analytes from miscellaneous matrices such as Fe_3O_4@metal–organic frameworks (MOFs) composites, Fe_3O_4@-covalent organic frameworks (COFs), magnetic molecularly imprinted and magnetic carbon materials.[13]

Department of Chemistry, Central Tehran Branch, Islamic Azad University, 1467686831, Tehran, Iran. E-mail: dr.manoochehri@yahoo.com; Fax: +98 2188385798; Tel: +98 9127242698

† Electronic supplementary information (ESI) available. See DOI: 10.1039/d0ra05408a

MOFs are classified as multifunctional microporous materials formed from metal ions and organic ligands through coordinate bonds. Tailorable chemistry, large specific surface areas, tunable cavities and good stability are the special features of MOFs, which has made this new type of scaffolds suitable for the incorporation of magnetic nanoparticles, providing versatile and efficient MSPE adsorbents.[13] Some adsorbents that provide selective separation and concentration of trace amounts of Be in natural water resources are silica gel,[14] activated carbon,[15] anion exchange resin,[16] salicylate chelating resin[17] and mixed micelle mediated extraction.[18]

Herein, a magnetic MOF for preconcentration of Be(II) was synthesized. The material is obtained from magnetite (Fe_3O_4) nanoparticles that were modified with 2-amino-5,8-dihydroxy-1,4-naphthoquinone (ADHNQ) and then reacted with terephthalic acid and iron(III) chloride to form the metal–organic framework of the type MIL-53(Fe) capable of extracting Be(II).

2 Experimental

2.1 Reagents and instrumentation

Benzen-1,4-dicarboxylic acid (H_2BDC), (3-chloropropyl)-triethoxysilane (3-CPTS), 2-amino-5,8-dihydroxy-1,4-naphthoquinone (ADHNQ), toluene, triethylamine, ammonium hydroxide (28% w/v), tetraethyl orthosilicate (TEOS), methanol, ethanol, *N*,*N*-dimethylformamide (DMF), acetone, $FeCl_3$, $(NH_4)_2$-$Fe(SO_4)_2 \cdot 6H_2O$, NaOH, HCl, H_2SO_4 and HNO_3, were supplied by Merck (Darmstadt, Germany) or Fluka (Seelze, Germany). Stock solution (1000 mg L^{-1}) of Be(II) was purchased from Merck. All the other solutions were daily prepared using distilled water.

2.2 Instrumentation

Be(II) determination was performed using a FAAS instrument model AA-680 Shimadzu (Japan) consisting an acetylene/nitrous oxide flame and a Be hollow cathode lamp with wavelength of 234.9 nm. Manufacturer's manual was used to set up the instrument. A digital 827 WTW Metrohm pH-meter composed of a combined glass-calomel electrode (Herisau, Switzerland) was employed for the pH measurements. Fourier transform infra-red (FT-IR) analysis carried out on a Bruker spectrophotometer model IFS-66. Elemental analysis of the nanoadsorbent was conducted using an EA112 flash elemental analyzer (Thermo Finnigan, Okehampton, UK). Scanning electron microscopy (SEM) study was performed on a KYKY-3200 instrument (Beijing, China). Magnetic features of the nanoadsorbents were recorded on a vibrating sample magnetometer (VSM) (AGFM/VSM 117 3886 Kashan, Iran). A Bahr STA-503 instrument (Behrthermo, Germany) was used for thermogravimetric analysis (TGA). Surface analysis was explored by nitrogen adsorption–desorption method employing a Micromeritics ASAP 2010 instrument. X-ray diffraction (XRD) analysis was conducted on a Philips-PW 12C diffractometer (Amsterdam, The Netherlands) using Cu Kα radiation.

2.3 Synthesis of the magnetic nanoadsorbent

MNPs@SiO_2 nanoparticles (NPs) was prepared according to the literatures[19–21] and the detailed information were provided in ESI.† For functionalization, in brief 1.0 g silica-coated magnetite NPs (Fe_3O_4@SiO_2) was addedto 75 mL dried toluene, and then 1.0 g 3-CPTES was added to the mixture and the reaction continued at 130 °C for 18 h under the reflux condition. Thereafter, the fabricated solid product was magnetically isolated from the reaction medium and it was washed with 50 mL ethanol three times and then dried at vacuum oven at 50 °C (Fig. 1a). For fabricating ADHNQ-functionalized MNPs, 1.0 g Fe_3O_4@SiO_2@3-CPTES was suspended in 150 mL 1 : 1 v/v methanol–TEA and then 0.25 g ADHNQ was added to the mixture. Afterwards, the mixture was heated under the reflux condition for 24 h (Fig. 1a). Ultimately, the final product was magnetically separated and washed with methanol and acetone several times and then dried in vacuum oven at 50 °C.

Fe_3O_4@SiO_2@ADHNQ@MIL-53(Fe) was fabricated *via* solvothermal method.[22] Briefly, 3.0 mmol H_2BDC was dissolved in 10 mL DMF containing 0.25 g Fe_3O_4@SiO_2@ADHNQ and the mixture was sonicated for 20 min. Thereafter, 3.0 mmol ferric chloride was dissolved in another vial that contains 5.0 mL DMF *via* sonication. Afterwards, the two mixture were mixed in a 50 mL Teflon lined stainless-steel autoclave, and the reaction was performed at 150 °C during 2 h. After the completion of the reaction, the temperature of mixture was allowed to decrease down to the room temperature. The Fe_3O_4@SiO_2@ADHNQ/MIL-53(Fe) was magnetically separated and washed with 3 × 30 mL deionized (DI) water and then 3 × 25 mL ethanol, and finally it was dried. The synthesis of Fe_3O_4@SiO_2@ADHNQ/MIL-53(Fe) was confirmed by FT-IR spectroscopy, SEM, elemental analysis, XRD, and VSM techniques. The same process was applied for the synthesis of MIL-53(Fe) in the absence of MNPs.

2.4 Extraction procedure

In brief, pH of samples were adjusted at 6.4 utilizing 0.25 mol L^{-1} NH_3 and HCl solutions. Thereafter, 32 mg Fe_3O_4@SiO_2@ADHNQ/MIL-53(Fe) nanoadsorbent was dispersed to the sample solution and it was stirred for 6.5 minutes. Afterwards, the nanosorbent was isolated magnetically and the supernatant solution was subjected to FAAS to determine the sorption%. For elution, the nanoadsorbent was dispersed in 1.0 mL of a solution containing 0.6 mol L^{-1} HNO_3 and the resultant mixture was stirred for 13.5 minutes. Finally, the mixture was separated using magnet and the supernatant was subjected to FAAS to determine recovery%.

2.5 Real sample and certified reference material preparation

The new method was utilized to a certified reference sample (NIST-SRM 1640), Cu–Be alloy and three different water samples (seawater river water and well water). The seawater (Caspian Sea, North of Iran), river water (Karaj, Iran) and well water (Karaj, Iran) samples were filtered into cleaned polyethylene bottles and their pH was adjusted to 6.4 before the extraction procedure. Acid digestion procedure was conducted to digest Cu–Be alloy sample. In this regard, 0.4 g of the sample was transferred into a 50 mL beaker and 5 mL 50% v/v HNO_3 was added to dissolve the alloy and finally it was diluted up to 100 mL using a volumetric flask and the pH of resulting solution was adjusted to 6.4 before extraction process.

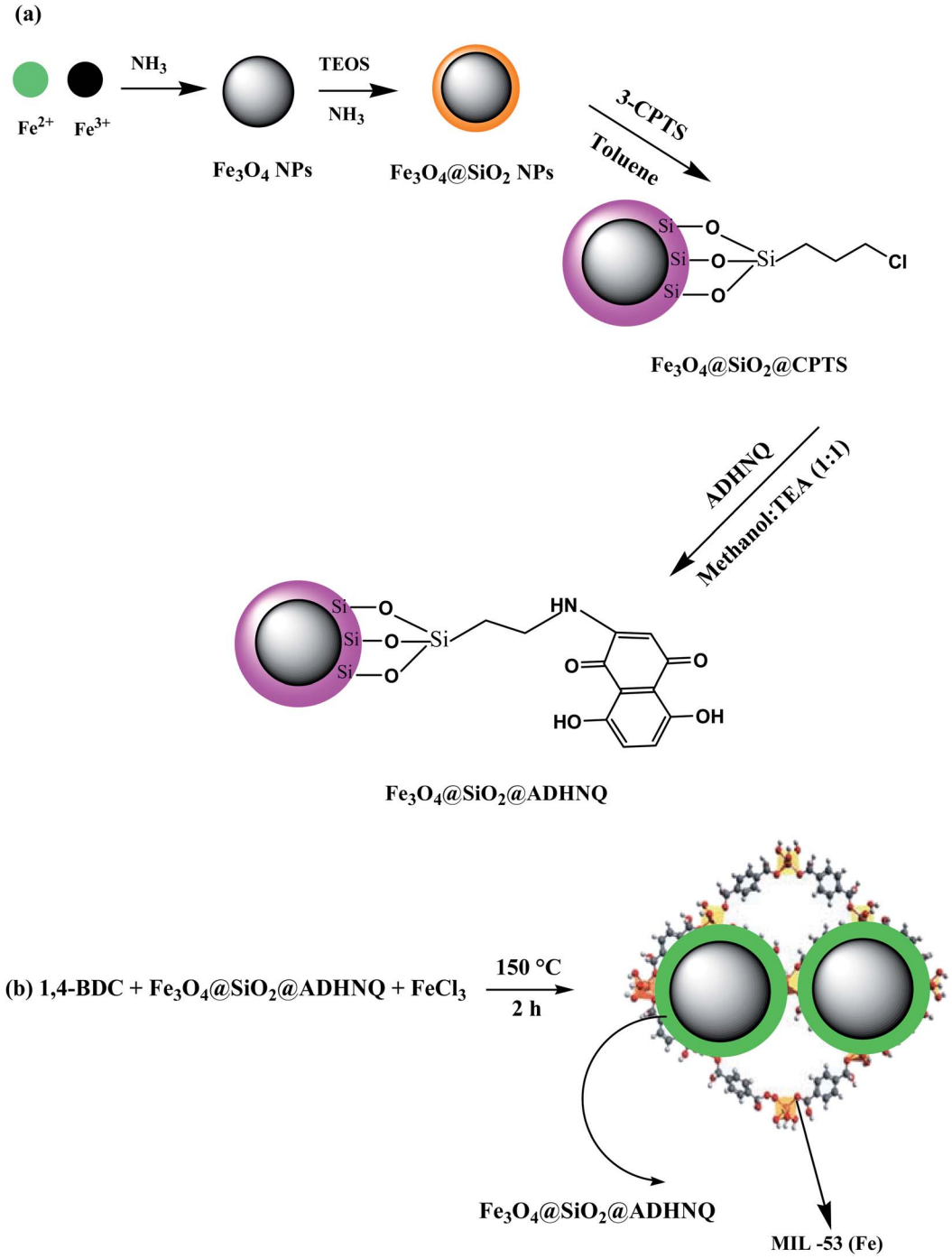

Fig. 1 (a) A scheme for the synthesis of $Fe_3O_4@SiO_2@ADHNQ$ and (b) $Fe_3O_4@SiO_2@ADHNQ/MIL-53(Fe)$ nanocomposite.

3 Results and discussion

3.1 Characterization of nanoadsorbent

The fabricated $Fe_3O_4@SiO_2@ADHNQ/MIL-53(Fe)$ sorbent at first was characterized by FT-IR spectroscopy (Fig. 2). The absorption bands at 583 cm^{-1}, 1014 cm^{-1}, 1168 cm^{-1}, 3370 cm^{-1}, 1389 cm^{-1}, 1503 cm^{-1}, 1598 cm^{-1}, and 1669 cm^{-1} were attributed to (Fe–O), (Si–O–Si), (C–N), (O–H), (C–OH), (C–O), (C=C) and (C=O), respectively, confirmed the presence of $Fe_3O_4@SiO_2@ADHNQ$ in MIL-53(Fe) structure and also proved the synthesis of $Fe_3O_4@SiO_2@ADHNQ/MIL-53(Fe)$. Elemental analysis of $Fe_3O_4@SiO_2@ADHNQ/MIL-53(Fe)$ was conducted to

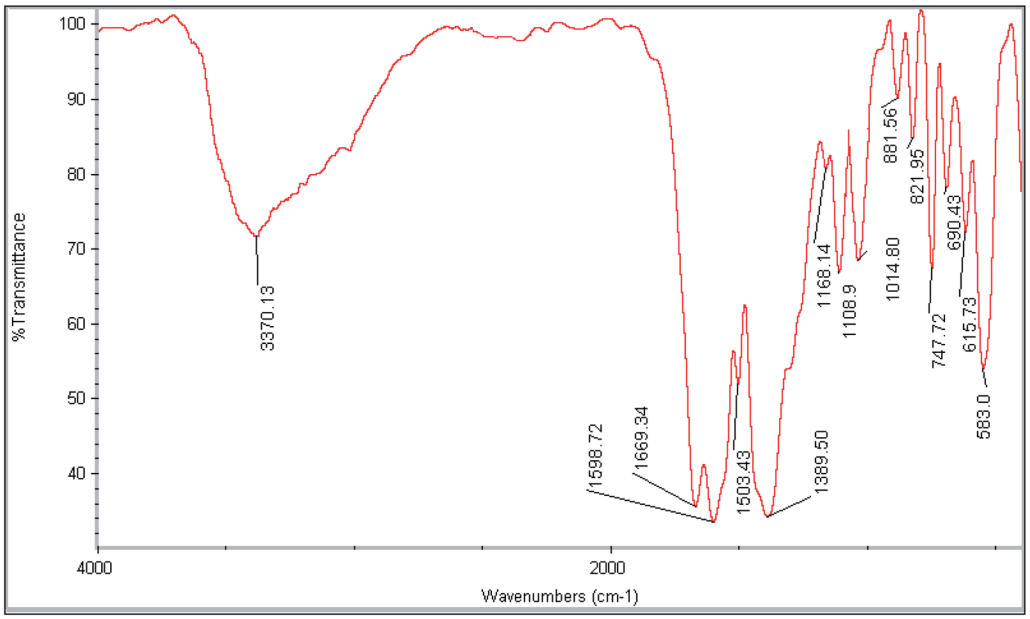

Fig. 2 FT-IR spectrum of Fe_3O_4@SiO_2@ADHNQ/MIL-53(Fe) nanoadsorbent.

determine the elements of nanocomposite. The results revealed 37.5% C, 1.7% H, and 3.5% Nin the structure of Fe_3O_4@SiO_2@ADHNQ/MIL-53(Fe) and confirmed the successful synthesis of nanoadsorbent.

To explore the surface morphology of Fe_3O_4@SiO_2@ADHNQ and Fe_3O_4@SiO_2@ADHNQ/MIL-53(Fe), SEM analysis was conducted. As depicted in Fig. 3a, Fe_3O_4@SiO_2@ADHNQ NPs are spherical with a mean diameter of about 50 nm. After functionalization, as can be seen in Fig. 3b, an increase in the particle size of Fe_3O_4@SiO_2@ADHNQ was observed (200 nm) which can be attributed to the coating of these particles with a MIL-53(Fe) layer.

The magnetic features of magnetite, Fe_3O_4@SiO_2@ADHNQ and Fe_3O_4@SiO_2@ADHNQ/MIL-53(Fe) were explored at ambient temperature with a VSM system and the obtained curves are exhibited in Fig. 4. The saturation magnetization for magnetite, Fe_3O_4@SiO_2@ADHNQ and Fe_3O_4@SiO_2@ADHNQ/MIL-53(Fe) was 65, 35.6 and 19.7 emu g^{-1}, respectively. Thus, this nanoadsorbent can be easily separated from the solution during DMSPE process with an external magnet due to their superparamagnetic and high saturation magnetization.[22]

The surface of the as-fabricated and reused Fe_3O_4@SiO_2@ADHNQ/MIL-53(Fe) were analyzed using BET N_2 adsorption–desorption method to obtain the specific surface area and pore volume of this sorbents. Accordingly, the surface and pore volume of as-fabricated Fe_3O_4@SiO_2@ADHNQ/MIL-53(Fe) was 21 m^2 g^{-1} and 0.022 cm^3 g^{-1}, respectively. The surface and pore volume of five times used Fe_3O_4@SiO_2@ADHNQ/MIL-53(Fe) was 18 m^2 g^{-1} and 0.016 cm^3 g^{-1}, respectively. The decrease in the surface and pore volume of the nanoadsorbent can be related to the possible damage of Fe_3O_4@SiO_2@ADHNQ/MIL-53(Fe) after reusing.

The structure of as-fabricated and reused Fe_3O_4@SiO_2@ADHNQ/MIL-53(Fe) were analyzed by XRD technique (Fig. 5).

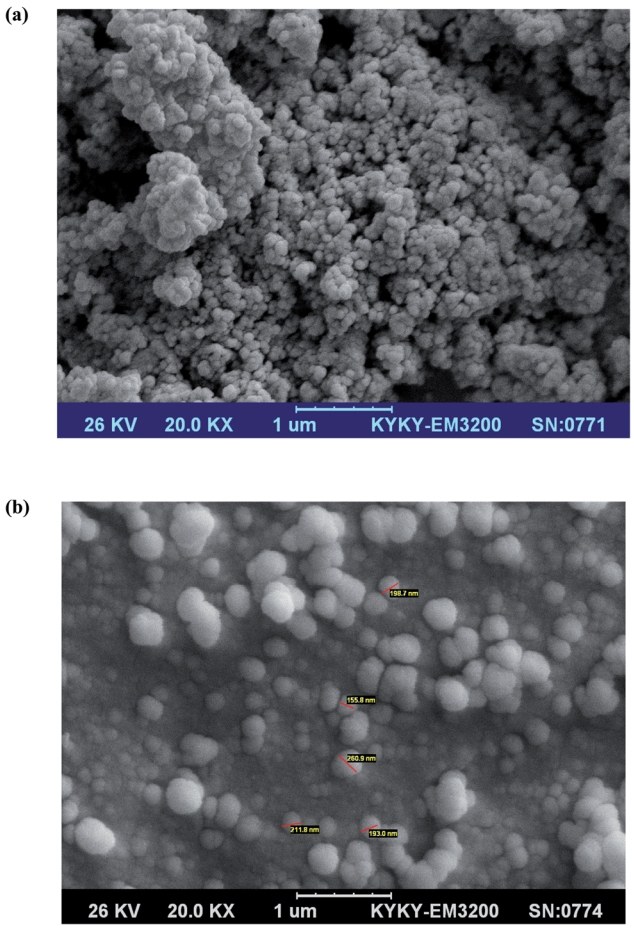

Fig. 3 SEM image of (a) Fe_3O_4@SiO_2@ADHNQ NPs and (b) Fe_3O_4@SiO_2@ADHNQ/MIL-53(Fe).

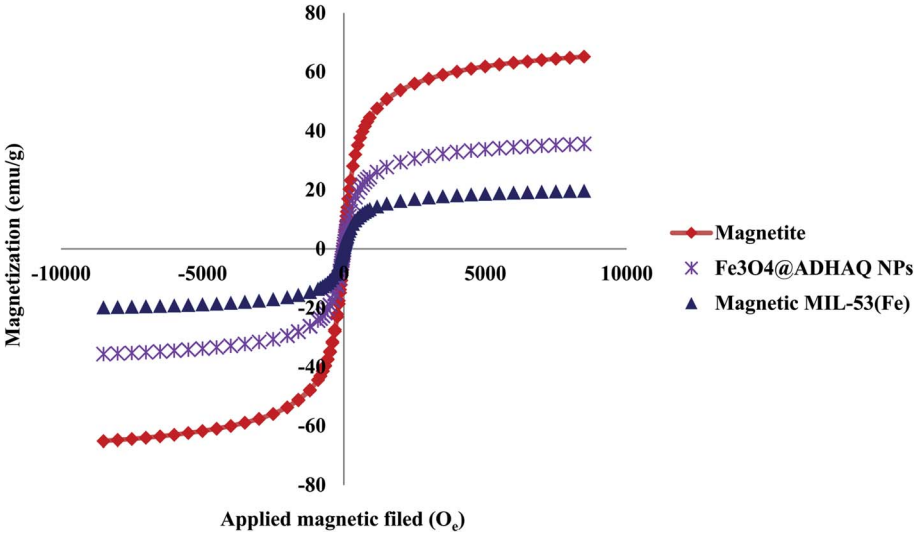

Fig. 4 VSM curves of the magnetite, Fe_3O_4@SiO_2@ADHNQ NPs and Fe_3O_4@SiO_2@ADHNQ/MIL-53(Fe) nanocomposite.

The diffraction peaks at $2\theta = 9.2°$, 12.6°, 17.6°, 18.9°, and 25.4° are related to the MIL-53(Fe) backbone.[22] The diffraction peaks at $2\theta = 30.3°$, 35.6°, 57.3°, and 62.0° are corresponded to MNPs and confirm the structure of Fe_3O_4@SiO_2@ADHNQ/MIL-53(Fe). The same XRD pattern was observed for 5-times used nanoadsorbent with a slight decrease in the peak's intensity which can be related to the partial damage of Fe_3O_4@SiO_2@ADHNQ/MIL-53(Fe) after reusing.

The thermal behavior of as-fabricated and reused Fe_3O_4@SiO_2@ADHNQ/MIL-53(Fe) were explored by TGA technique (Fig. 6). The as-fabricated and reused nanoadsorbents exhibited the same thermal behavior. A sharp losing weight between 270 °C and 420 °C was observed and the total weight loss up to 800 °C for as-fabricated and reused Fe_3O_4@SiO_2@ADHNQ/MIL-53(Fe) was 86.5% and 91.5%, respectively. This difference can be attributed to the partial damage of Fe_3O_4@SiO_2@ADHNQ/MIL-53(Fe) after reusing.

3.2 Optimization

The experimental design methodology enables the analyst to select the best optimum conditions with minimum numbers of experiment, minimum of time and cost consumption. In order to achieve the best extraction performance, the main parameters affecting the extraction of the suggested DMSPE method were evaluated and optimized through the central composite design (CCD). CCD is composed of a two level factorial design (2^f), star points ($2f$) and center points that are located at the center of the experimental region (C_0). Center points are performed to establish the experimental error and the star points are located at $\pm\alpha$ from the center of experimental domain and provide wider extremes for the low and high settings of factors.[23] Response surface methodology (RSM) has been extensively employed for the effective modeling and specify of main factors involved the DMSPE. Desirability function is the predominant and most approach applied to access the best agreement between the two responses based on the mathematical models constructed in response surface methodology. In this regards, the effect of following variable were explored and optimized: (a) pH; (b) Fe_3O_4@SiO_2@ADHNQ/MIL-53(Fe) dosage; (c) adsorption time; (d) eluent type; (e) eluent concentration; (f) eluent volume; (g) elution time. Based on the number of experiments for a CCD assay ($N = 2^f + 2f + C_0$, N: number of experiments; f: number of variables and C_0: number of

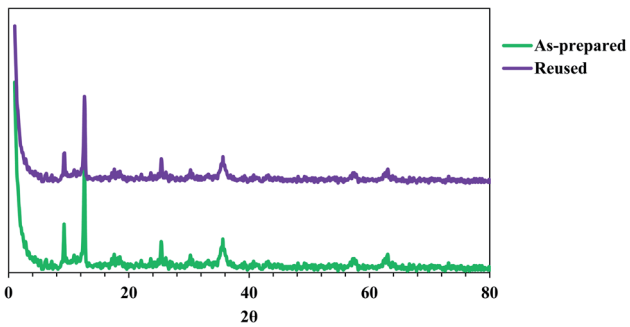

Fig. 5 XRD patterns of as-prepared Fe_3O_4@SiO_2@ADHNQ/MIL-53(Fe) and reused Fe_3O_4@SiO_2@ADHNQ/MIL-53(Fe).

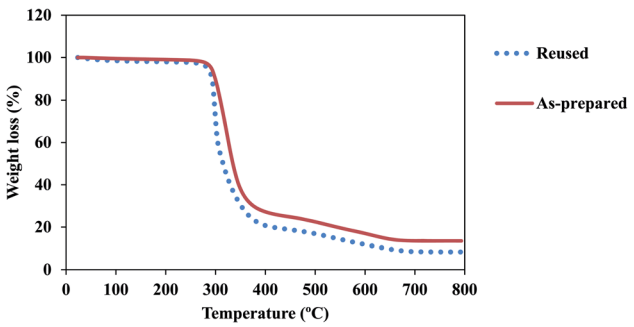

Fig. 6 TGA curves of as-prepared Fe_3O_4@SiO_2@ADHNQ/MIL-53(Fe) and reused Fe_3O_4@SiO_2@ADHNQ/MIL-53(Fe).

replicates in center point), f and C_0 were set at 3 and 5, respectively and hence 19 tests were designed for each step (sorption and elution). Two replicates were conducted for each test and the average was considered as a suitable response. The results of the experimental design for each step along with their corresponding response were presented in Fig. 7 and 8, Table 1S.† The points with high desirability were depicted with red color and low desirability with green colors. From evaluating the result, the best extraction conditions were: (a) optimum pH: 6.4; (b) Fe_3O_4@SiO_2@ADHNQ/MIL-53(Fe) dosage: 32 mg; (c) adsorption time: 6.5 min; (d) eluent type: HNO_3; (e) eluent concentration: 0.6 mol L^{-1}; (f) eluent volume: 1.0 mL; (g) desorption time: 13.5 min.

3.3 Effect of interfering

The effect of potentially interfering ions on the recoveries of the Be(II) ions was also investigated. The obtained results were summarized in Table 2S.† The coexisting ions did not show considerable effect on the recovery of Be(II). The results revealed that the nanoadsorbent possessed high selectivity toward Be(II) ions in the presence of other interfering ions. The presence hydroxyl moieties on the surface of nanoadsorbent impart the selective interaction to Be(II) ions. According to the hard and soft acid–base theory, hard acids such as Be(II) ions react more efficiency with the ligands consisting oxygen moieties (such as naphthoquinone) as the hard bases.[18]

3.4 Sorption capacity and effect of sample volume

Under the optimized condition, sorption capacity of Fe_3O_4@SiO_2@ADHNQ/MIL-53(Fe) towards Be(II) was evaluated. To this aim, the adsorption capacity of Fe_3O_4@SiO_2@ADHNQ/MIL-53(Fe) toward Be(II) was explored utilizing 100 mL standard solution and calculated by using equation:

$$SC = \frac{(C_0 - C_e)V}{q}$$

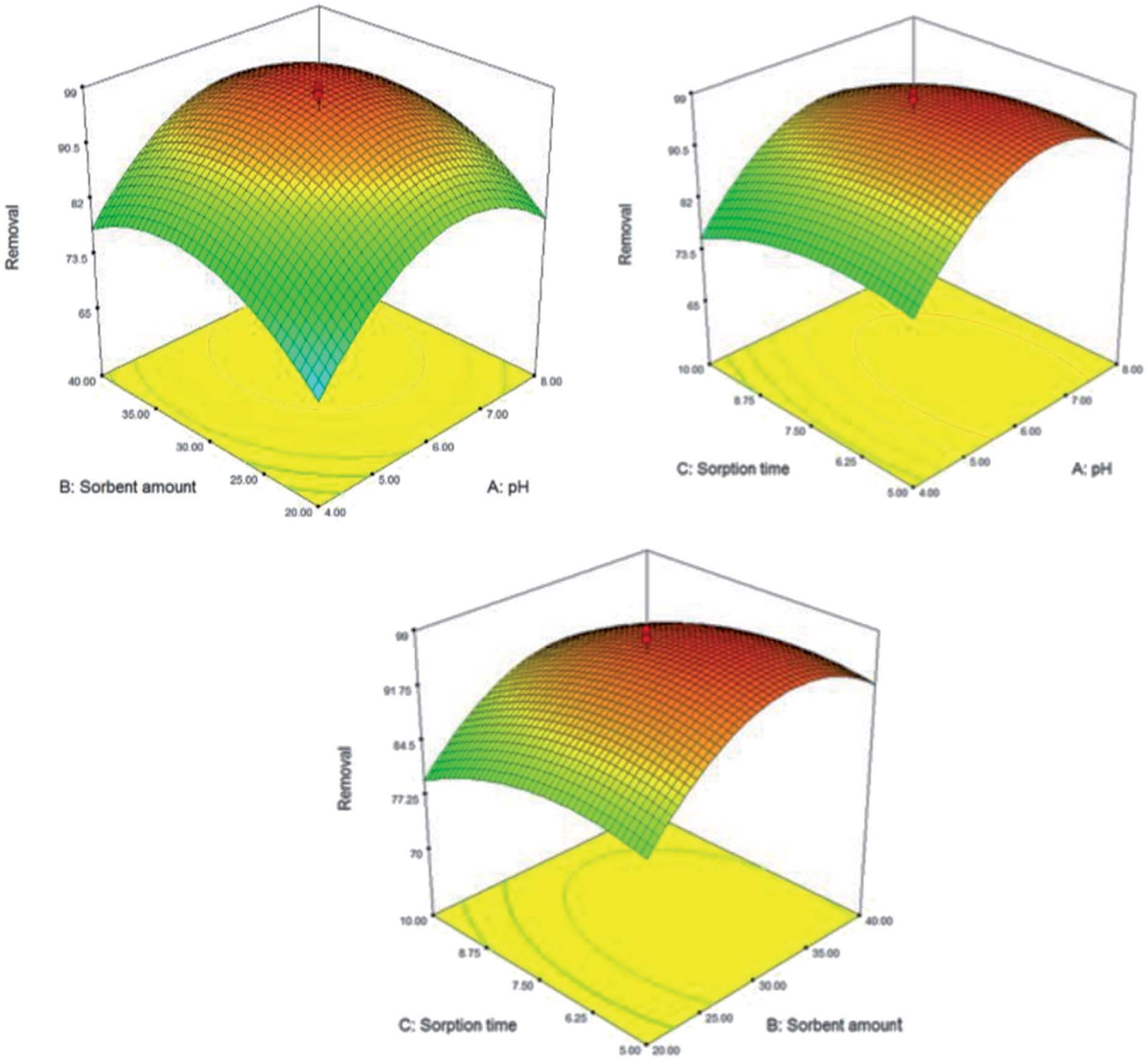

Fig. 7 3D response surface plots of the sorption step.

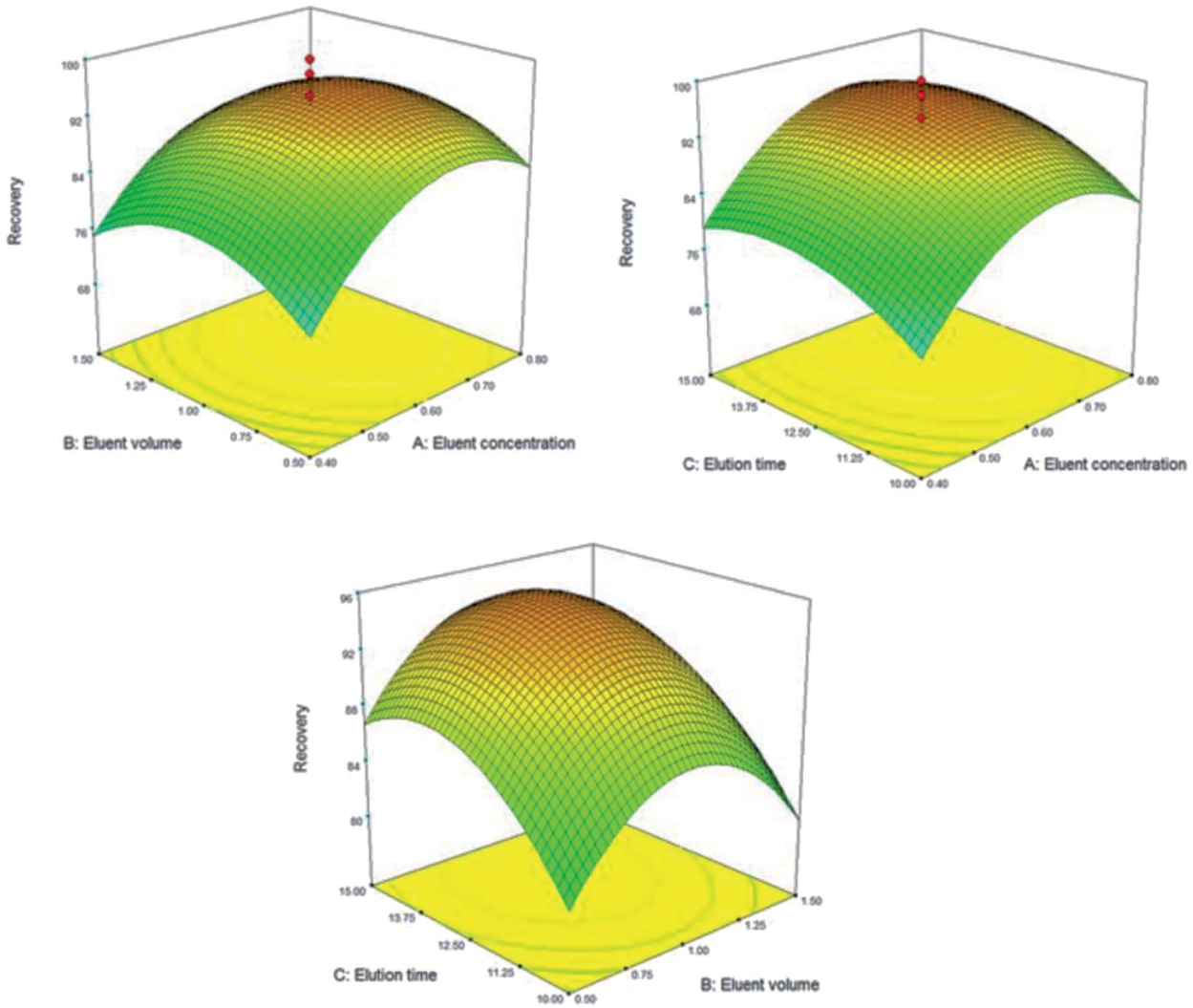

Fig. 8 3D response surface plots of the elution step.

where, SC represents the sorption capacity per gram of nanoadsorbent, C_0 and C_e are the initial and equilibrium concentration of Be(II) (mg L^{-1}), q is the weight of nanoadsorbent (mg) and V is the volume of Be(II) solution (L). Based on the achieved result, the maximum sorption capacity was calculated as 284 mg g^{-1}. This high SC can be attributed to the porous structure of Fe_3O_4@SiO_2@ADHNQ/MIL-53(Fe) increasing its adsorption capacity.

The effect of the volume of sample on the recovery of Be(II) ions was also explored in the range of 50–500 mL. The results illustrated that the increase in the sample volume up to 350 mL leads to an enhancement in the recovery, while for the sample volumes more higher 350 mL the recovery decreases. Hence, Fe_3O_4@SiO_2@ADHNQ/MIL-53(Fe) nanoadsorbent provides a preconcentration factor of 350 regarding to the sample (350 mL) and eluent (1 mL) volumes.

3.5 Analytical features

Under the optimized conditions, analytical features of the DMSPE-combined FAAS method such as limit of detection, dynamic linear range, accuracy and precision were evaluated. An excellent linear relationship between the absorption and

Table 1 Determination of beryllium in certified reference material

	Concentration				
CRM	Analyte	Certified	Found	Recovery (%)	Error (%)
NIST SRM 1640	Beryllium	34.94 (μg L^{-1})	34.3 ± 2.8	98.2	−1.8

Table 2 Determination of beryllium in different real samples (mean ± SD)[a]

Sample	Real value	Added value	Found value[b]	Recovery (%)
Well water	N.D.[d]	5.0	4.9 ± 0.32[c]	98
Caspian sea water	1.7 ± 0.05[c]	5.0	6.75 ± 0.48[c]	101
River water	N.D.[d]	5.0	4.45 ± 0.10[c]	89
Cu–Be alloy	0.64[b] ± 0.04	1.0	1.58 ± 0.10	94

[a] Standard deviation ($n = 3$). [b] w/w%. [c] For water samples concentration are based on μg L^{-1}. [d] N.D.: not detected.

Be(II) concentration was achieved from 0.2–100 ng mL^{-1} with r^2 value equal to 0.9965. The limit of detection (LOD) was calculated to be 0.07 ng mL^{-1} based on $3S_b/m$, where S_b is the standard deviation of 10 replicates blank signal, m = slop of calibration plot. The obtained LOD is much lower than the maximum permitted level of Be(II) in water. The relative standard deviation (RSD) for 5 replicate extraction and determinations of 30 ng mL^{-1} Be(II) was investigated and found to be lower than 5.8, indicating the good precision of the proposed method. In the next step, the accuracy of the developed method was explored by estimation Be(II) level in NIST SRM 1640 certified reference material. The obtained amount was in well agreement with the certified value and the results confirm the excellent accuracy of the method, as summarized in Table 1.

3.6 Analytical applicability

In the next step, the analytical applicability of the DMSPE combined with FAAS method was evaluated for extraction and determination of Be(II) in seawater, well water, river water and Cu–Be alloy samples. The relative recoveries and standard deviations were presented in Table 2. As summarized in Table 2, the recoveries for the Be(II) were ranged from 89 to 101% with standard deviation lower than 10% for three replicate tests. These result indicated the method could be very promising for determination of Be(II) in real samples without significant matrix effects.

4 Conclusions

Herein, for the first time Fe_3O_4@SiO_2@ADHNQ/MIL-53(Fe) nanoadsorbent was successfully fabricated and then was DMSPE adsorbent for the extraction and preconcentration of Be(II) at trace levels. Fe_3O_4@SiO_2@ADHNQ/MIL-53(Fe) exhibited high selectivity to Be(II) due to its functionalization with ADHNQ molecules. Moreover, the porous structure of Fe_3O_4@SiO_2@ADHNQ/MIL-53(Fe) increases its adsorption capacity. The proposed DMSPE method is quick, easy, cost-effective, and has low detection limit (0.07 ng mL^{-1}) and excellent dynamic linear range (0.2–100 ng mL^{-1}) compared to other reports (Table 3S, ESI†). A high maximum sorption capacity equal to 284 mg g^{-1} was obtained. The accuracy of the developed method was explored by estimation Be(II) level in NIST SRM 1640 certified reference material. The obtained amount (34.3 ± 2.8 μg L^{-1}) was in well agreement with the certified value (34.94 μg L^{-1}) and the results confirm the excellent accuracy of the method. Ultimately, to explore the feasibility of the method, it was applied for quick extraction and determination of Be(II) in three different water samples and an Cu–Be alloy and satisfactory result was obtained. These results proved that the DMSPE combined FAAS can be considered as an alternative adsorbent for extraction and determination of Be(II) from real samples.

Conflicts of interest

The authors declare that they have no conflict of interest.

References

1 J. Devoy, M. Melczer, G. Antoine, A. Remy and J. F. Heilier, Validation of a standardised method for determining beryllium in human urine at nanogram level, *Anal. Bioanal. Chem.*, 2013, **405**(25), 8327–8336.
2 H. K. Fouad, M. S. Atrees and W. I. Badawy, Development of spectrophotometric determination of beryllium in beryl minerals using chrome Azurol S, *Arabian J. Chem.*, 2016, **9**, S235–S239.
3 A. Mayer and N. Hamzeh, Beryllium and other metal-induced lung disease, *Curr. Opin. Pulm. Med.*, 2015, **21**(2), 178–184.
4 P. Ashtari, K. Wang, X. Yang and S. J. Ahmadi, Preconcentration and separation of ultra-trace beryllium using quinalizarine-modified magnetic microparticles, *Anal. Chim. Acta*, 2009, **646**(1–2), 123–127.
5 E. Yavuz, Ş. Tokalıoğlu and Ş. Patat, Dispersive solid-phase extraction with tannic acid functionalized graphene adsorbent for the preconcentration of trace beryllium from water and street dust samples, *Talanta*, 2018, **190**, 397–402.
6 N. Khan, T. G. Kazi, M. Tuzen and M. Soylak, A multivariate study of solid phase extraction of beryllium(II) using human hair as adsorbent prior to its spectrophotometric detection, *Desalin. Water Treat.*, 2015, **55**(4), 1088–1095.
7 E. Hosseini, M. Chamsaz and M. Ghorbani, A Novel Ultrasonic Assisted Dispersive Solid Phase Microextraction for Preconcentration of Beryllium Ion in Real Samples Using CeO_2 Nanoparticles and its Determination by Flame Atomic Absorption Spectrometry, *Eurasian J. Anal. Chem.*, 2017, **13**, 1–10.
8 M. Chamsaz, K. Samghani, M. H. Arbab-Zavar and T. Heidari, Spectrofluorimetric Determination of Beryllium

by Mean Centering of Ratio Spectra, *J. Fluoresc.*, 2016, **26**(4), 1401–1405.

9 A. Nawrocka, M. Durkalec, J. Szkoda and M. Kmiecik, Determination of trace and essential elements in honey by quadrupole-inductively coupled plasma-mass spectrometry, *58Method Development*, 2016, p. 52.

10 S. R. Yousefi, F. Shemirani, M. R. Jamali and M. Salavati-Niasari, Extraction and preconcentration of ultra trace amounts of beryllium from aqueous samples by nanometer mesoporous silica functionalized by 2,4-dihydroxybenzaldehyde prior to ICP OES determination, *Microchim. Acta*, 2010, **169**(3–4), 241–248.

11 S. D. Harvey, R. B. Lucke and M. Douglas, Rapid separation of beryllium and lanthanide derivatives by capillary gas chromatography, *J. Sep. Sci.*, 2012, **35**(20), 2750–2755.

12 Y. Wen, L. Chen, J. Li, D. Liu and L. Chen, Recent advances in solid-phase sorbents for sample preparation prior to chromatographic analysis, *TrAC, Trends Anal. Chem.*, 2014, **59**, 26–41.

13 L. Lian, X. Zhang, J. Hao, J. Lv, X. Wang, B. Zhu and D. Lou, Magnetic solid-phase extraction of fluoroquinolones from water samples using titanium-based metal–organic framework functionalized magnetic microspheres, *J. Chromatogr. A*, 2018, **1579**, 1–8.

14 W. Szczepaniak and A. Szymanski, Sorption and preconcentration of trace amounts of beryllium from natural waters on silica gel with immobilized morin prior to its determination by ETA-AAS method, *Chem. Anal.*, 1996, **41**, 193–199.

15 T. Okutani, Y. Tsuruta and A. Sakuragawa, Determination of a trace amount of beryllium in water samples by graphite furnace atomic absorption spectrometry after preconcentration and separation as a beryllium–acetylacetonate complex on activated carbon, *Anal. Chem.*, 1993, **65**, 1273–1276.

16 A. Afkhami, T. Madrakian, A. A. Assl and A. A. Sehhat, Spectrophotometric determination of beryllium in water samples after micelle-mediated extraction preconcentration, *Anal. Chim. Acta*, 2001, **437**, 17–22.

17 J. Kubova, V. Nevoral, V. Stresko and Z. Fresenius, Determination of beryllium trace contents in mineral waters after preconcentration on a chelating ion-exchanger, *J. Anal. Chem.*, 1994, **348**, 287–290.

18 A. Beiraghi, Cloud-point formation based on mixed micelles for the extraction, preconcentration and spectrophotometric determination of trace amounts of beryllium in water samples, *Anal. Sci.*, 2007, **23**, 527–531.

19 A. A. Asgharinezhad, N. Jalilian, H. Ebrahimzadeh and Z. Panjali, A simple and fast method based on new magnetic ion imprinted polymer nanoparticles for the selective extraction of Ni(II) ions in different food samples, *RSC Adv.*, 2015, **5**(56), 45510–45519.

20 S. Sadeghi and E. Aboobakri, Magnetic nanoparticles with an imprinted polymer coating for the selective extraction of uranyl ions, *Microchim. Acta*, 2012, **178**, 89–97.

21 M. Mehraban, M. Manoochehri and F. A. Taromi, Trace amount determination of Cd(II), Pb(II) and Ni(II) ions in agricultural and seafood samples after magnetic solid phase extraction by MIL-101 (Cr)/phenylthiosemicarbazide-functionalized magnetite nanoparticle composite, *New J. Chem.*, 2018, **42**(21), 17636–17643.

22 N. Jalilian, H. Ebrahimzadeh and A. A. Asgharinezhad, A nanosized magnetic metal–organic framework of type MIL-53(Fe) as an efficient sorbent for coextraction of phenols and anilines prior to their quantitation by HPLC, *Microchim. Acta*, 2019, **186**(9), 597.

23 H. Ebrahimzadeh, N. Shekari, Z. Saharkhiz and A. A. Asgharinezhad, Simultaneous determination of chloropheniramine maleate and dextromethorphan hydrobromide in plasma sample by hollow fiber liquid phase microextraction and high performance liquid chromatography with the aid of chemometrics, *Talanta*, 2012, **94**, 77–83.